Original article

Ukr Neurosurg J. 2024;30(3):38-51
doi: 10.25305/unj.306363

Comparison of the effects of photodynamic exposure with the use of chlorine E6 on glioblastoma cells of the U251 line and human embryonic kidney cells of the HEK293 line *in vitro*

Volodymyr D. Rozumenko [1], Larysa D. Liubich [2], Larysa P. Staino [2], Diana M. Egorova [2], Andrii V. Dashchakovskyi [1], Victoriya V. Vaslovych [3], Tatyana A. Malysheva [3]

[1] Department of Neurooncology and Pediatric Neurosurgery, Romodanov Neurosurgery Institute, Kyiv, Ukraine
[2] Tissue Culture Laboratory, Department of Neuropathomorphology, Romodanov Neurosurgery Institute, Kyiv, Ukraine
[3] Department of Neuropathomorphology, Romodanov Neurosurgery Institute, Kyiv, Ukraine

Received: 17 June 2024
Accepted: 17 July 2024

Address for correspondence*:*
Larysa D. Liubich, Tissue Culture Laboratory, Romodanov Neurosurgery Institute, 32 Platona Maiborody st., Kyiv, 04050, Ukraine, e-mail: lyubichld@gmail.com

Malignant gliomas of the brain are a global medical and social problem with a trend toward a steady increase in morbidity and mortality rates. A method that enables the visual identification of tumor tissue and simultaneously selectively destroys it is photodynamic therapy, which involves the introduction of a photosensitizer (PS) followed by its activation at a certain wavelength of light. The selectivity of the accumulation of PS in the tumor tissue of the malignant gliomas is one of the key issues in the problem of increasing the effectiveness of photodynamic therapy.

Objective: to compare the effects of photodynamic exposure using PS chlorin E6 on human glioblastoma (GB) cells of the U251 line and non-malignant human embryonic kidney cells of the HEK293 line.

Material and methods. Groups of cell cultures were formed depending on the conditions of cultivation and exogenous influence: 1) control - cultivated in a standard nutrient medium (*Modified Eagle's Medium (*MEM)) with L-glutamine, 1 mmol of sodium pyruvate, 10% fetal bovine serum) and experimental: 2) cultivated under the conditions of adding chlorin E6 (concentrations 1.0 and 2.0 μg/ml); 3) cultivated on a nutrient medium without the addition of PS and exposed to laser irradiation (LI) (λ=660 nm, power in the range 0.4-0.6 W, dose in the range 10-75 J/cm^2, continuous or pulse mode); 4) cultured under conditions of chlorin E6 addition and subsequent exposure to LI (power in the range 0.4-0.6 W, dose in the range 10-75 J/cm^2, continuous or pulse mode). After exposure to the specified experimental factors, dynamic observation with microphotographic registration was performed for 24 h, followed by microscopic and micrometric studies (number of viable cells, total number of cells, mitotic index (MI,%)).

Results. PS chlorin E6 is incorporated into the cytoplasm of cells of U251 and HEK293 cell lines, the intensity of fluorescence is comparable. Upon exposure to chlorin E6 (1.0 and 2.0 μg/ml), cytodestructive and antimitotic effects are increased in a dose-dependent manner in the culture of human GB cells of the U251 line. The cytodestructive effect of chlorin E6 on cell cultures of the HEK293 line is less pronounced, but the antimitotic effect is comparable in both types of cell cultures. Under the influence of LI, cytodestructive and antimitotic effects increase in a dose-dependent manner in the culture of human GB cells of the U251 line. The level of cytodestructive and antimitotic effects is significantly lower in the cultures of non-neoplastic HEK293 cells. The most significant drop in the mitotic activity of GB U251 cells (~100%) was recorded at the lowest LI dose of 25 J/cm^2, power of 0.6 W in pulse mode. For HEK293 cells, the most significant decrease in mitotic activity (~80%) was recorded at LI with a power of 0.6 W and dose of 75 J/cm^2 in continuous mode. Under the combined effect of chlorin E6 (1 and 2 μg/ml, pre-incubation of 4 h) and LI in different modes, the viability of tumor cells in U251 culture decreases in a dose-dependent manner; the smallest dose of LI to achieve the maximum cytotoxic effect is 25 J/cm^2, with a power of 0.6 W in pulse mode when using chlorin E6 at a concentration of 2 μg/ml. The specified characteristics of photodynamic exposure do not cause irreversible effects in HEK293 cultures (reference cells).

Conclusions. An effective mode of photodynamic exposure to achieve a cytodestructive and antimitotic effect in the culture of human GB cells of the U251 line, which is relatively safe for non-malignant cells, has been established: the combined application of a laser irradiation dose of 25 J/cm^2, with a power of 0.6 W in pulse mode during the preliminary incubation of the cell culture with chlorin E6 at a concentration of 2 μg/ml for 4 h.

Key words: *laser irradiation; photosensitizer; malignant gliomas; glioblastoma; U251; HEK293; mitotic index*

Introduction

The treatment of malignant gliomas (MG) remains a serious challenge globally, despite research into the causes of their occurrence and mechanisms of progression. Malignant brain tumors are a global medical and social problem, with a trend towards increasing incidence and mortality rates (primarily due to the progression of MG) [1-5]. Traditional surgical approaches with ad oculus imaging may leave unnoticed tumor cells in the zone of invasive spread that migrate over significant distances. Consequently, MG recurrence often occurs near the marginal (perifocal) area of the surgical cavity [6]. Additionally, in functionally critical areas of the brain, the radical surgical removal of tumors is impossible. Photodynamic therapy (PDT), a two-stage process involving the introduction of a photosensitive chemical agent (photosensitizer) followed by its intraoperative activation at a certain wavelength of light, is a method that allows to identify the tumour tissue visually intraoperatively and simultaneously destroy it with maximum clarity (objectively) [6, 7].

The principle of PDT is based on the cytotoxic effects induced by the generation of singlet molecular oxygen and free radicals by the activated photosensitizer (PS), which trigger photochemical reactions in the tumor cells, leading to the destruction of basic cytoskeletal proteins. The tumor tissue is believed to have a higher affinity for the PS, which selectively incorporates into neoplasm cells [8, 9]. The simultaneous use of fluorescence-guided surgery and PDT allows for the visualization and targeted destruction of tumor cells [9-11], optimizing the determination of tumor spreading boundaries for maximal removal [12].

Analysis of clinical trial data suggests that using PDT as an adjunct treatment for MG immediately after maximal resection is safe, reduces the risk of recurrence by targeting residual tumor cells in the resection cavity, and improves patient survival and quality of life [10,13-21]. The lack of information on the development of resistance to multiple PDT sessions suggests the potential for repeated treatment of tumor cells that were not removed during surgery.

Since the efficiency of photodynamic damage to sensitized cells is determined by the intracellular concentration of the PS, its localization within the cell, photochemical activity, and the dose of laser irradiation (LI), developing *in vitro* experimental models to evaluate PDT effectiveness is a relevant task. Photosensitizers must cross the blood-brain barrier, selectively localize in tumor tissue without significant accumulation in healthy tissues, exhibit maximum cytotoxic activity against tumor cells, and be rapidly excreted from the body [22, 23]. In researching PS, the focus is on compounds of natural origin, one of which is chlorin E6 — a second-generation PS, representing natural pigments obtained from green algae. Chlorin E6 is combined with polyvinylpyrrolidone (a biocompatible polymer that imparts water solubility to the hydrophobic chlorin E6), which promotes tumor accumulation due to the increased permeability of defective tumor vessels and reduced lymphatic drainage [24]. The selective accumulation of the PS in MG tumor tissue is one of the key issues for improving the effectiveness of PDT.

Objective: to compare the effects of photodynamic therapy using the photosensitizer chlorin E6 on human GB cells of the U251 line and non-malignant human embryonic kidney cells of the HEK293 line.

Materials and Methods

The study was conducted on cultures of human glioblastoma (GB) cells of the U251 line and human embryonic kidney HEK293 cell line. Cryopreserved cell samples (kindly provided by the "Cell Bank of Human and Animal Tissue Lines," R.E. Kavetsky Institute of Experimental Pathology, Oncology and Radiobiology, NAS of Ukraine, Kyiv) were thawed in a water bath for 30 min at 38°C, suspended in 10 ml of Modified Eagle's Medium (MEM) with L-glutamine (Biowest, France) without serum, and centrifuged (5 min at 1000 rpm, MICROmed CM-3). The cell pellet was suspended in MEM medium with L-glutamine (1 mmol sodium pyruvate, 10% fetal calf serum (Biowest, France)), and placed in culture plastic flasks (25 cm^3, Cellstar, Germany) at a concentration of $0.1 \cdot 10^6$ cells/8 ml of the culture medium. Cultures were maintained in a CO_2 incubator (Nuve, Turkey) under standard conditions (95% humidity, 37°C, 5% CO_2). The culture medium was changed every three days. Dynamic observation with microphotoregistration was performed using a "Nikon S-100" inverted microscope (Japan).

Cells in the amount of $2 \cdot 10^6$ were transferred to plastic Petri dishes (d = 35 mm, Sarstedt, Germany) on coverslips pre-coated with polyethyleneimine (Sigma-Aldrich, GmbH, Germany), the culture medium (2 ml) was added, and cells were cultured until a monolayer (75-80%) was achieved.

To investigate the immediate effects of chlorin E6 in the cell culture with a formed monolayer, the PS was added at a concentration of 1 or 2 μg/ml. To investigate the direct effects of LI, plates with cultures were placed under the vertical fiber-optic laser output (h = 5 cm) of the "LIKA-surgeon" device ("Photonics-Plus", Ukraine) and irradiated with uniform coverage of the monolayer surface area with light beams (λ – 660 nm) under various modes (power range - 0.4 - 0.6 W, dose (exposure - surface energy density relative to the irradiated surface area) - 10 - 75 J/cm^2, continuous or pulse mode). The exposure time of LI to the cell culture depended on the applied power and mode (the maximum duration of irradiation was 240 s for LI 0.6 W, 75 J/cm^2, pulse mode). The irradiated cultures were kept at room temperature during this time, while the cultures of the comparison groups were kept under similar conditions. To study the combined effects of chlorin E6 and LI, the PS was added to the cell culture with a formed monolayer (at concentrations of 1 and 2 μg/ml) and held in a CO_2 incubator (Nuve, Turkey) for 4 h, after which the cultures were irradiated under various modes as indicated above. The variants of experimental exposure combinations on cell cultures are presented in the ***Table***.

After exposure to the specified experimental factors, the cultures were kept in a CO_2 incubator (Nuve,

This article contains some figures that are displayed in color online but in black and white in the print edition.

Turkey) and subjected to dynamic observation with microphotoregistration using an inverted microscope "Nikon S-100" (Japan) for 24 h. Microphotoregistration of fluorescence was conducted using an Axiophot microscope (Opton, Germany) with fluorescent filters (λ - [500-680] nm).

To determine the cytotoxic effects of chlorin E6 and laser irradiation, the cell cultures were exposed to various research conditions with the addition of a vital dye (0.2% trypan blue solution (Merck, Germany)) to the culture medium, and the growth of cultures was observed using an inverted microscope for 24 h.

For further analysis, cell culture groups were formed based on cultivation conditions and exogenous exposure: 1) control - cultured in a standard nutrient medium (MEM with L-glutamine, 1 mmol sodium pyruvate, 10% fetal calf serum) and experimental: 2) chlorin E6 addition (concentrations of 1.0 and 2.0 μg/ml); 3) cultured in a nutrient medium without addition of a PS and exposed to LI (power - 0.4–0.6 W, dose - 10–75 J/cm², continuous or pulse mode); 4) cultured with the addition of chlorin E6 and exposed to LI (power - 0.4–0.6 W, dose - 10–75 J/cm², continuous or pulse mode).

Table. Conditions for experimental exposure to cell cultures

№	Exposure conditions				Number of cell cultures	
					U251	HEK293
1	Control				10	9
2	Chlorin E6			1,0 μg/ml	9	13
				2,0 μg/ml	10	14
3	Laser irradiation (LI)	0,4 W	10 J/cm2	continuous mode	3	3
				pulse mode	3	3
			25 J/cm2	continuous mode	3	3
				pulse mode	3	3
		0,6 W	10 J/cm2	continuous mode	3	3
				pulse mode	3	3
			25 J/cm2	continuous mode	7	3
				pulse mode	7	3
			50 J/cm2	continuous mode	3	3
				pulse mode	3	3
			75 J/cm2	continuous mode	3	3
				pulse mode	3	3
4	Chlorin E6 (1 μg/ml) + LI	0,4 W	10 J/cm2	continuous mode	3	3
				pulse mode	3	3
			25 J/cm2	continuous mode	3	3
				pulse mode	3	3
		0,6 W	10 J/cm2	continuous mode	3	3
				pulse mode	3	3
			25 J/cm2	continuous mode	3	3
				pulse mode	3	3
	Chlorin E6 (2 μg/ml) + LI	0,4 W	10 J/cm2	continuous mode	3	3
				pulse mode	3	3
			25 J/cm2	continuous mode	3	3
				pulse mode	3	3
		0,6 W	10 J/cm2	continuous mode	3	3
				pulse mode	3	3
			25 J/cm2	continuous mode	7	3
				pulse mode	7	3
			50 J/cm2	continuous mode	3	3
				pulse mode	3	3
			75 J/cm2	continuous mode	3	3
				pulse mode	3	3

Cell cultures were fixed in 10% neutral formalin (Bio-Optica, Italy) and stained with hematoxylin and eosin by the Carazzi method. Microscopic examination and photoregistration of cytological preparations were carried out using a light-optical photomicroscope "Nikon Eclipse E200" (Japan). In each preparation, the structural features of experimental cultures were compared with the control ones. The analysis included cell shape, the presence and branching of processes, chromatin structure and distribution, nuclear morphology, and intercellular interactions.

Quantitative studies of experimental cultures compared to the control were conducted in 10 representative fields of view using a standard measuring scale (object micrometer). Morphometric analysis was performed by processing digital images of cultures in 10 randomly selected fields of view (0.04 mm^2) for each sample at the same magnification (800x) using ImageView software (2020). The test area determined the number of viable cells, the total number of cells, and the number of cells in the mitotic division state. The mitotic index (MI, %) was calculated as the percentage of cells undergoing mitosis per 100 cells.

Statistical analysis of the obtained data was performed using a licensed statistical software package (StatSoft Inc., 2022). The normality of data distribution was determined by the Shapiro-Wilk test. Non-parametric methods of variation statistics were applied (Kruskal-Wallis rank-based ANOVA for multiple comparisons of several independent groups, Mann-Whitney U-test for pairwise comparison of independent groups, and Wilcoxon test for pairwise comparison of dependent groups over time). Data are presented per unit of test area (0.04 mm^2) as (M±m), where M is the arithmetic mean, m is the standard deviation from the arithmetic mean. Differences were considered statistically significant at $p<0.05$.

Results and Discussion

As an *in vitro* model of MG, we used cultures of human GB cells of the U251 line, which was obtained from a malignant human brain GB tumor by explantation. The cell type of the tumor was identified as pleomorphic/astrocytoid [25].

Human GB cells of the U251 line in culture demonstrated typical growth dynamics: starting from the formation of chains and dense monolayer cell conglomerates alongside individual cells without distinct signs of differentiation (with narrow cytoplasm and moderate nuclear polymorphism) and astrocytic cells with processes during the 1st day after explantation ***(Fig. 1A)*** to the expansion of the monolayer of tumor cells (large in size with distinct contours, clear cytoplasm, large nucleus, astrocytic structure, unipolar, triangular, rhomboid, polygonal shape with elongated processes) on the 5^{th}-7^{th} day ***(Fig. 1B)***. At the stage of confluent growth, the cultures showed reticular proliferation of densely packed tumor cells with high polymorphism. Histological preparations in the growth zone of the cultures revealed 2-3 tumor cells in the mitotic division stage within the field of view ***(Fig. 1C)***. On the 7^{th} day of cultivation in the control cultures of U251 cell line, in the growth zones of undifferentiated tumor cells, the mitotic index (MI) averaged (0.88±0.05) %.

To compare the efficiency of photodynamic effects on non-tumor tissues, we used the HEK293 cell line - an immortalized line artificially created by transforming a culture of human embryonic kidney cells with fragments of adenovirus 5 DNA [26]. HEK293 cells have an epithelial-like structure and form monolayer cultures. They usually have a flattened elongated shape with well-defined cell boundaries and high adhesion. HEK293 cells do not express tissue-specific genes but do express markers of renal progenitor cells, neuronal cells, and adrenal cells [27]. The presence of specific gene products and mRNA, typically detected in neurons, along with the potential for induced synaptogenesis, the functionality of endogenous neuron-specific voltage-dependent channels, and responses to various agonists involved in neuron signaling, support considering HEK293 as cells with a neuronal phenotype [27]. HEK293 cells have a complex phenotype due to a heterogeneous unstable atypical karyotype: they have two or more copies of each chromosome, with a modal chromosome number of 64-hypotriploid karyotype (containing more than two copies (diploid), but less than three); three copies of the X chromosome and four copies of chromosomes 17 and 22) [28]. The average number of chromosomes and chromosomal aberrations vary in HEK293 cells and their derivatives, as well as in HEK293 cells from different cell banks/laboratories [27].

In our studies, in the first 24 h, we observed an adherent population of small, mostly slightly rounded cells growing dispersed, as well as a small number of polygonal and distinctly elongated cells ***(Fig. 2A)***.

When cultured for 5-7 days, HEK293 cells formed a continuous monolayer of epithelial-like structure, arranged quite densely, with a large number of intercellular contacts. Most cells exhibited regular, balanced shapes, with occasional round, cylindrical, and polygonal forms. The cells had dense cytoplasm and a centrally located large oval-round nucleus containing 1-2 (rarely 3) nucleoli ***(Fig. 2B)***. A significant number of proliferatively active cells were observed ***(Fig. 2D)***. On the 7^{th} day of cultivation in control cultures of HEK293 cells line in the growth zones, the MI averaged (0.61±0.07)%. In the trypan blue test, a small proportion of spontaneously degenerated cells were noted ***(Fig. 2C)***.

Effects of chlorin E6 in cultures of U251 and HEK293 cell lines. After applying chlorin E6 at a concentration of 1 μg/mL for 24 h in U251 cell line cultures, a thinning of the growth zone was observed, with the appearance of large lacunae in the cellular monolayer ***(Fig. 3A)***. Among intact cells, diffusely located dystrophic or necrobiotically altered tumor cells were found, characterized by reduction of processes, rounded cytoplasm with signs of progressive lipid and hydropic dystrophy, and hyperchromatic nuclei. Some tumor cells turned into shadow cells or "naked" nuclei, forming small clusters. The number of cells in the mitotic state decreased to 1-2 in the field of view (MI averaged (0.71±0.08) %, $p=0.14$ compared to control, Mann-Whitney U-test). Blocked forms of K-mitoses were noted among the figures of mitotic division of tumor cells.

With an increased concentration of chlorin E6 (2 μg/ml), within just 6 h, there was noticeable thinning of U251 cell culture masses due to retraction of the growth zone and reduction of processes in damaged cells. After

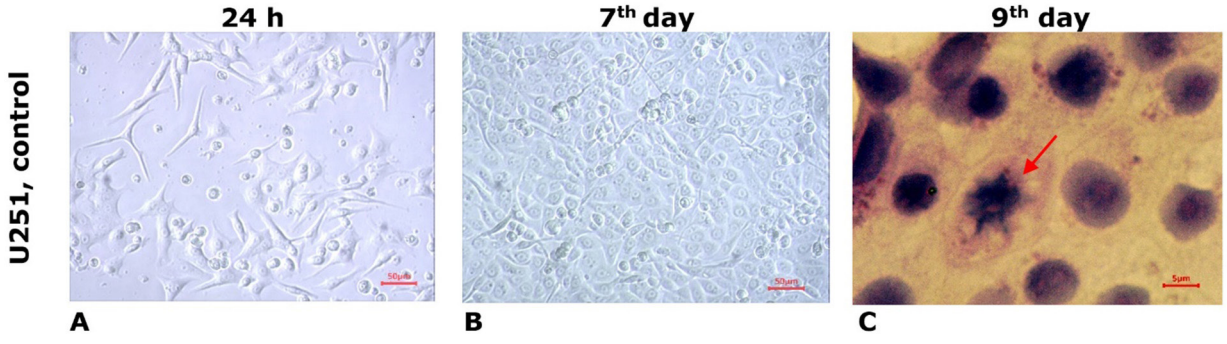

Fig. 1. Microphotos of human GB U251 cell cultures grown in standard culture medium (control). Light microscopy, unstained culture (A, B); staining with hematoxylin and eosin (C). The arrow indicates a cell in the mitotic phase (prophase)

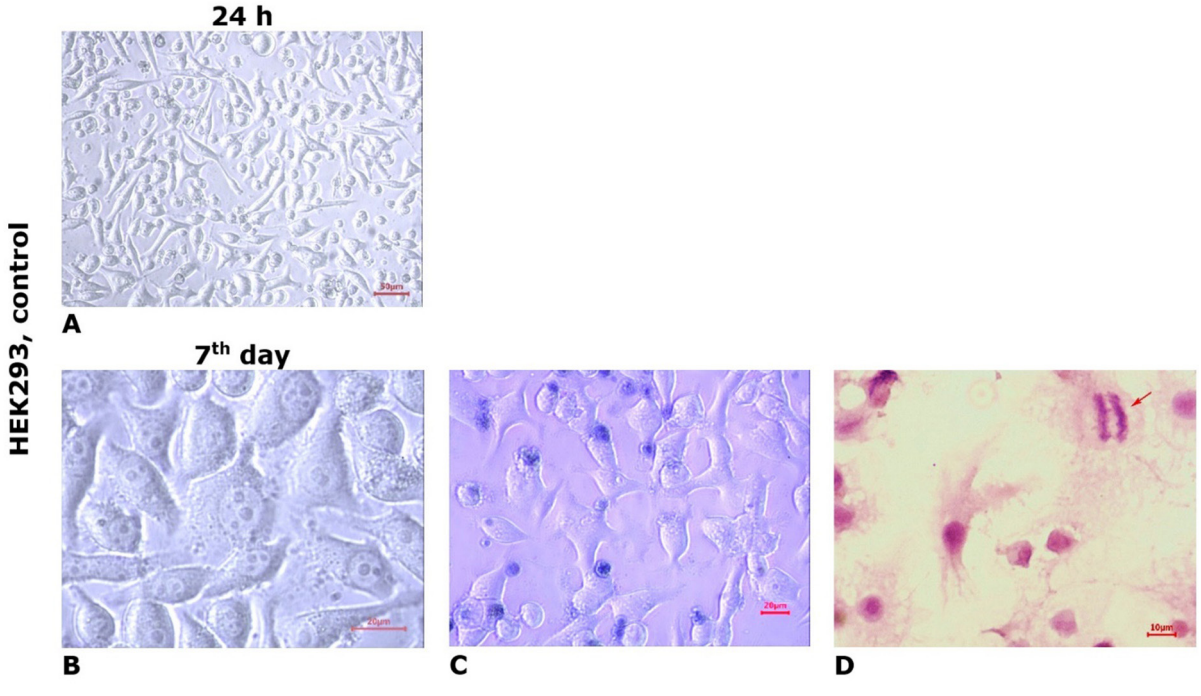

Fig. 2. Microphotos of HEK293 cell line cultures grown in standard culture medium (control). Light microscopy, unstained culture (A, B); staining with trypan blue vital dye (C); staining with hematoxylin and eosin (D). The arrow indicates a cell in the mitotic phase (anaphase)

24 h, intercellular adhesion was lost, leading to the formation of small and large lacunae in the monolayer of cells in the growth zone, dilution of cell masses, and desquamation of some dead cells. In some areas, the growth zone of U251 cells was almost completely depleted with only a few degenerated round-shaped cells remaining. Reticulated structures with degenerating cells (with cytoplasmic vacuolization and loss of processes) persisted in isolated areas ***(Fig. 3A)***. In the preserved areas of the growth zone monolayer, mitotic activity of some tumor cells was maintained (one cell in mitosis was observed in several fields of view, MI decreased to (0.15±0.02)%, $p=1\cdot10^5$ compared to control, p=0.04 compared with the value when exposed to chlorin E6 (1 μg/ml), Mann-Whitney U-test) ***(Fig. 4)***.

Unlike the U251 cell line, the growth zone of HEK293 cells remained intact 24 h after exposure to chlorin E6 at a concentration of 1 μg/ml. While cell density remained high, pathological changes were observed, including reduction of processes, cytoplasmic rounding, nuclear displacement to the periphery of the cytoplasm, and vacuolization ***(Fig. 3C)***. HEK293 cells maintained a low level of mitotic activity (MI was, on average, (0.33±0.04)%, p=0.04 compared to control, Mann-Whitney U-test). Increasing the concentration of chlorin E6 to 2 μg/ml had little effect on the HEK293 cell monolayer density but did result in an increase in the number of rounded cells with reduced processes, vacuolated cytoplasm, and decentered nuclei ***(Fig. 3C)***. A few mitotically active cells were observed in the growth

zone (MI decreased to (0.23±0.03)% ***(Fig. 4)***, p=0.01 compared to control, p=0.6 compared to the effect of chlorin E6 (1 μg/ml), Mann-Whitney U-test), among which pathological forms (asymmetric mitoses) were observed, leading to telophase disruption, resulting in the appearance of binucleated and multinucleated cells in the monolayer.

According to the data of fluorescence study, in experimental cultures of U251 and HEK293 cells, chlorin E6 accumulated in the cytoplasm, and the fluorescence intensity in different cell types was nearly identical ***(Figs. 3B, 3D)***, likely due to the heterogenous phenotype characteristics of HEK2 cells [27]. Other authors have reported localization of the photosensitizer in cytoplasmic organelles as well [29].

In contrast to cell lines U251 and HEK293, the fluorescence intensity of chlorin E6 incorporated into non-malignant rat brain cells (E14-16) was much weaker [30], which aligns with data regarding the higher affinity and selective accumulation of photosensitizers in tumor tissues [22].

Thus, the results of testing chlorin E6 exposure indicate a dose-dependent cytotoxic effect on tumor cells of the U251 line. Unlike the U251 cell line, HEK293 cell cultures did not experience such destruction of the growth zone when exposed to chlorin E6, as the majority of cells remained intact. However, the anti-mitotic effect of chlorin E6 was relatively comparable in both types of cell cultures.

Effects of laser irradiation at various modes on U251 and HEK293 cell line cultures

After 24 h of LI exposure (0.4 W power, 10 J/cm² dose, continuous mode), a retraction of the growth zone with the formation of lacunae of varying sizes and compaction of the tumor cell monolayer was observed in U251 cell cultures ***(Fig. 5A)***. Under the same conditions, HEK293 cell cultures did not exhibit significant monolayer disruption; the cells maintained characteristic sizes and shapes ***(Fig. 5C)***. Under pulse mode LI (0.4 W, 10 J/cm²), no additional changes were observed in both studied cell lines compared to previous observations ***(Fig. 5B)***.

Under LI exposure at 0.4 W, 25 J/cm² in continuous mode, further retraction of the growth zone occurred in cultures of cell line U251, with intact monolayer regions preserved ***(Fig. 5A)***. In HEK293 cell line cultures, no damage to the growth zone was detected under these conditions; the trypan blue test revealed a small number of degenerated cells ***(Fig. 5C)***. With LI (0.4 W, 25 J/cm²) in pulse mode, there was further compaction of the U251 cell monolayer, an increase in lacunae in the growth zone, and the number of degenerated cells ***(Fig. 5B)***, along with a significant reduction in mitotic activity (***Fig. 6A***; $p=3\cdot10^{-6}$ compared to control, p=0.007 compared to the indicator under continuous LI mode, Mann-Whitney U-test). No significant changes were observed in HEK293 cell line cultures under the same conditions ***(Figs. 6B, 6D)***.

Under higher power laser irradiation (0.6 W, 10 J/cm², continuous mode) in U251 cell cultures, a substantial reduction in the total number of cells in the monolayer was observed, with most cells rounding up and losing intercellular contacts, leading to the depletion of the growth zone ***(Fig. 5A)***. Meanwhile, the HEK293 cell monolayer did not undergo significant changes ***(Fig. 5C)***. Laser irradiation (0.6 W, 10 J/cm²) in pulse mode caused the destruction of the U251 cell growth zone: most cells had reduced processes and lost contacts with each other and the surface, leading to monolayer degradation with the formation of unformed cell aggregates and fragments ***(Fig. 6B)***. The mitotic activity of U251 cells was at a low level (***Fig. 6A***; $p=1\cdot10^{-6}$ compared to control, Mann-Whitney U-test). In HEK293 cell cultures under the same conditions, the appearance of pathologically altered cells was noted (with loss of characteristic shape and rounding), as well as the presence of binucleated cells and displacement of nuclei to the cytoplasm's periphery ***(Fig. 5D)***. The mitotic activity of HEK293 cells changed little ***(Fig. 6B)***, and the monolayer cell density slightly decreased compared to the control.

When exposed to LI (0.6 W, 25 J/cm², continuous mode), there was a significant reduction in the total number of U251 cells in the damaged growth zone, with large areas devoid of cells or containing only a few cells at different stages of degeneration ***(Fig. 5A)***. In cultures of the cell line HEK293 under the same conditions, nuclear displacement to the periphery of the cytoplasm was observed in most cells, with an increase in the number of rounded cells but without a loss in monolayer density or the overall cell count in the growth zone ***(Fig. 5C)***. LI (0.6 W, 25 J/cm²) in pulse mode intensified the destructive processes in U251 cell cultures ***(Fig. 5B)*** and practically eliminated mitotic activity (***Fig. 6A***; $p=3\cdot10^{-6}$ compared to control, p=0.34 compared to the index in continuous LI mode, Mann-Whitney U-test). In cultures of HEK293 cells under the same conditions, significant damage to the cell mass was not observed, and the monolayer density remained high, although the number of rounded degenerated cells increased ***(Fig. 5D)*** and mitotic activity indices significantly decreased (***Fig. 6B***; p=0.02 compared to control, p=0.27 compared to continuous LI mode, Mann-Whitney U-test).

Increasing the LI dose to 50 J/cm² in continuous mode at 0.6 W led to an increase in dystrophic and necrobiotic changes in the cells of U251 line and the appearance of a significant number of apoptotic bodies ***(Fig. 5A)***. Under the same conditions, LI (0.6 W, 50 J/cm²) in pulse mode intensified destructive processes in the U251 cell growth zone ***(Fig. 5B)***. Necrobiotic processes of spontaneous cell death affected most cells in the growth zone, and MI significantly decreased ($p=1\cdot10^{-6}$ compared to control, p=0.55 compared to the index of continuous LI mode, Mann-Whitney U-test). In HEK293 cell cultures under the same conditions, LI led to a reduction in cell density in the monolayer growth zone compared to control cultures (p<0.05, Mann-Whitney U-test, **Fig. 6B**). Cells maintained their characteristic shape, but vacuolization in the cytoplasm was observed ***(Fig. 5C, 5D)***, and mitotic activity significantly decreased (p=0.03, p=0.04 compared to control, Mann-Whitney U-test).

After exposure to a LI dose of 75 J/cm² (power 0.6 W) in both continuous and pulse modes, an increase in growth zone destruction and dystrophic and necrobiotic changes were observed in cultures of cell line U251 ***(Fig. 5A, 5B)***. In some areas, the growth zone was completely devastated with almost total cell destruction. Chromatin coagulation was observed in some cells, turning into a sharply basophilic

homogeneous mass (pyknosis), indicating membrane integrity disruption. Mitotic activity almost disappeared ($p=1 \cdot 10^{-6}$ compared to control, $p=0.41$ compared to the index in continuous LI mode, Mann-Whitney U-test). Cytological preparations of preserved areas of the growth zone recorded an increase in the proportion of pathologically altered cells with a large number of cell shadows and "bare nuclei" against a sharp decrease in the total cell count ***(Fig. 6A)***.

In HEK293 cell cultures, LI (0.6 W 75 J/cm²) in continuous mode led to the rounding and separation of cells in the dense monolayer, enlargement of nuclei, cytoplasmic vacuolization, decreased cell adhesion, and, consequently, disruption of the growth zone ***(Fig. 5C)***. LI with the same parameters in pulse mode led to vacuolization of HEK293 cells, loss of intercellular contacts, cell rounding, and lysis, which reduced the monolayer density ***(Fig. 5D).*** Mitotic activity was low

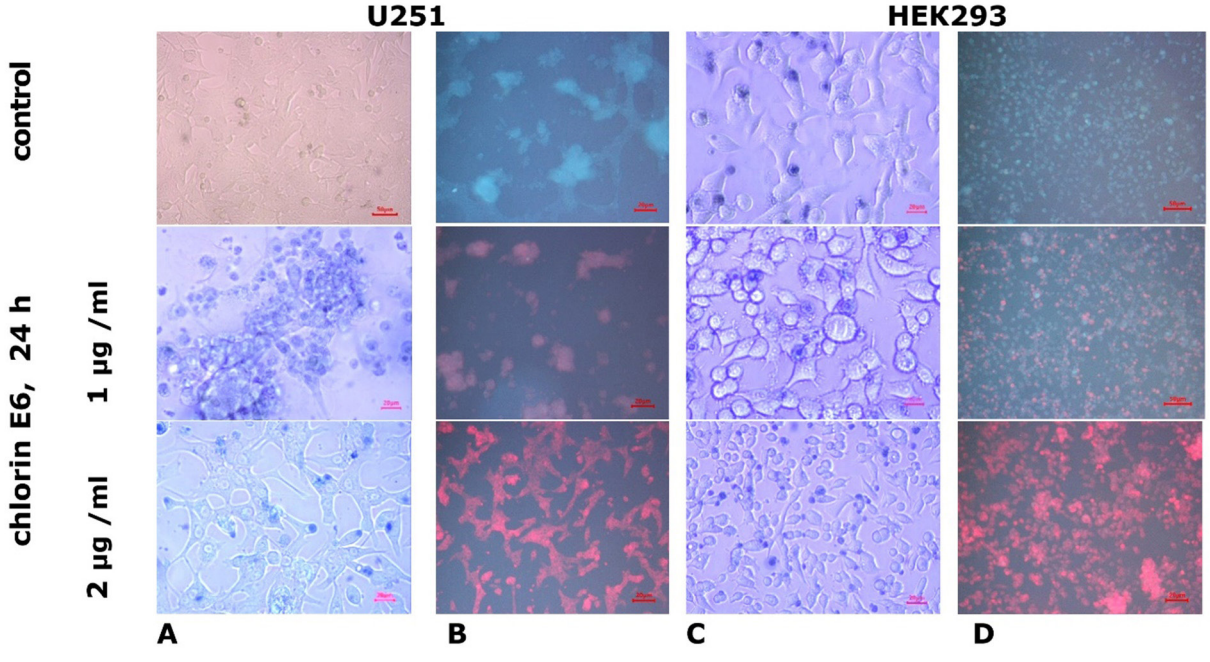

Fig. 3. Microphotos of U251 human glioblastoma cell cultures and HEK293 cell cultures grown in standard medium and after the addition of chlorin E6 at different concentrations. Light (A, C) and fluorescence (B, D) microscopy. Staining with trypan blue vital dye

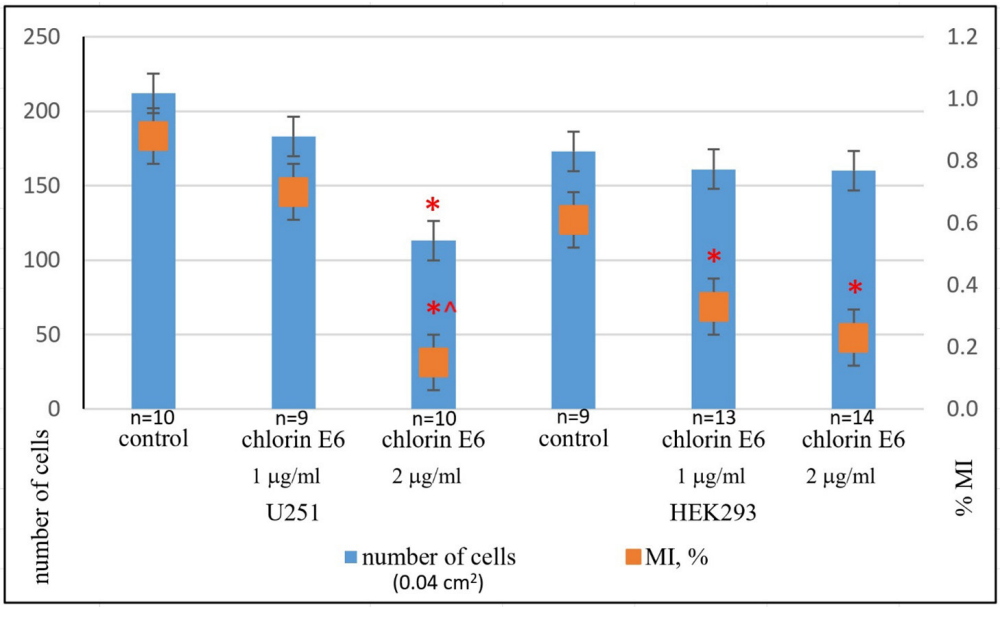

Fig. 4. Average number of cells and mitotic index (MI, %) in U251 human GB cell cultures and HEK293 cell cultures 24 h after the addition of chlorin E6 at different concentrations: * – $p<0.05$ compared to control; ^ – $p<0.05$ compared to chlorin E6 (1 μg/ml); Mann-Whitney U-test

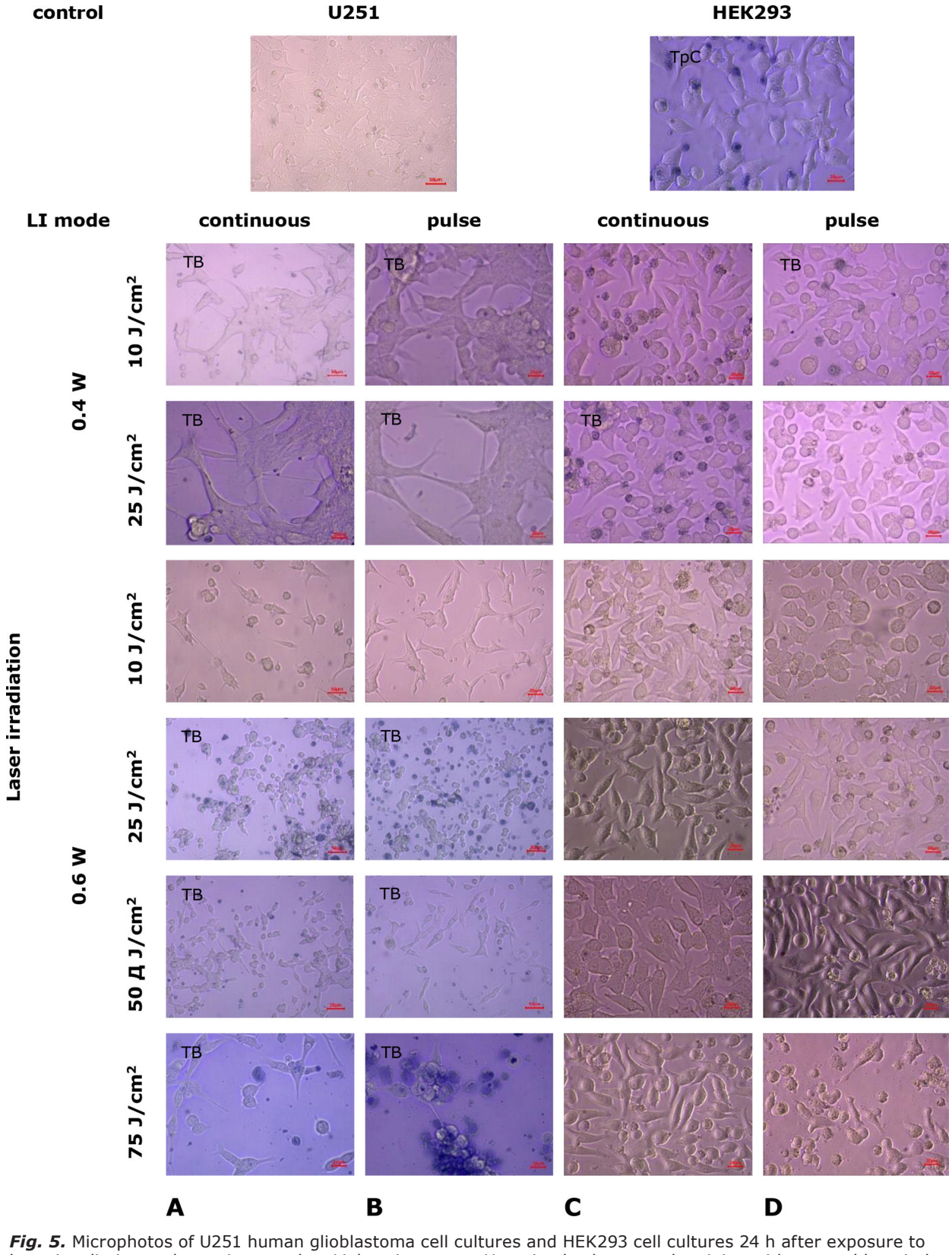

Fig. 5. Microphotos of U251 human glioblastoma cell cultures and HEK293 cell cultures 24 h after exposure to laser irradiation under various modes. Light microscopy. Unstained cultures and staining with trypan blue vital dye (TB)

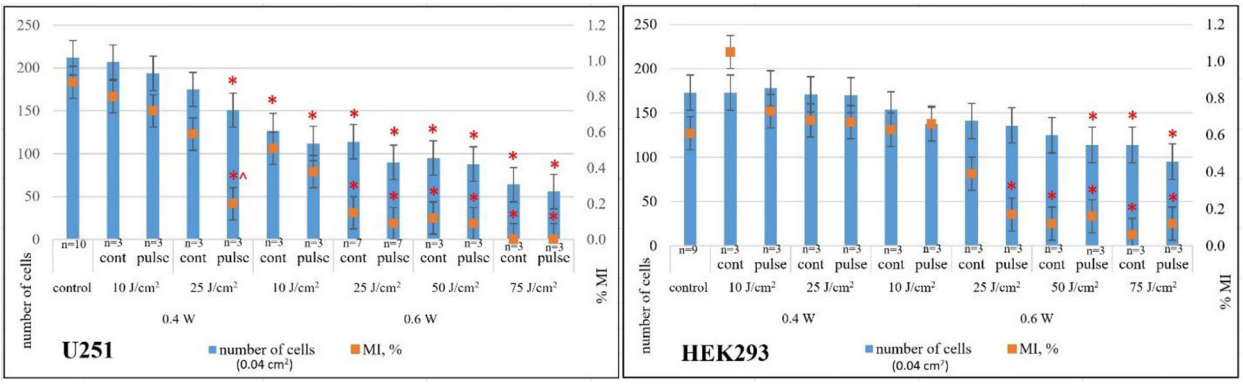

A B

Fig. 6. Average cell count and mitotic index (MI, %) in U251 human GB cell cultures (A) and HEK293 cell cultures (B) 24 h after laser irradiation under various modes: * - p<0.05 compared to control; ^ - p<0.05 compared to continuous mode of laser irradiation, Mann-Whitney U-test

(p=0.01 compared to control, p=0.58 compared to the index in continuous LI mode, Mann-Whitney U-test; ***Fig. 6B***).

Therefore, studies testing the effects of LI on U251 human GB cell cultures demonstrate a dose-dependent cytotoxic effect. Increasing the power from 0.4 to 0.6 W and the dose from 10 to 75 J/cm² in continuous mode leads to destructive changes in the growth zone's architectonics (from growth zone retraction with lacunae formation of varying sizes at the lowest LI parameters to severe destruction and significant cell mass depletion at the highest parameters). There was also a gradual decrease in mitotic activity of tumor cells and accumulation of necrobiotic changes up to irreversible degeneration with subsequent desquamation of dead cells. This effect tends to intensify with the same laser irradiation characteristics in pulse mode, significantly differing from the effect of laser irradiation at 0.4 W, 25 J/cm² (p=0.007, Mann-Whitney U-test).

In contrast to tumor cells of U251 line, the degree of LI influence in the applied modes on non-tumor cells of HEK293 line was significantly less: the first pathological changes of HEK293 line cells without changes in the growth zone were detected starting with LI power of 0.6 W (dose 10 J/cm²) in pulse mode, and significant monolayer density changes occurred with an increase in LI dose to 75 J/cm² in pulse mode.

Based on the dynamics of the mitotic activity indicator, it was found that the most significant reduction in U251 human GB cell culture was registered starting with laser irradiation power of 0.6 W (dose 25 J/cm²). In this mode, HEK293 cell cultures retained mitotic activity.

The most significant decrease in mitotic activity of U251 human GB cells (~100%) was recorded at a minimum LI dose of 25 J/cm², power 0.6 W in pulse mode ($p=3\cdot10^{-6}$ compared to control, p=0.34 compared to continuous LI mode, Mann-Whitney U-test; ***Fig. 6A***). For HEK293 cells, the most significant reduction in mitotic activity (~80%) was recorded at LI power 0.6 W (dose 75 J/cm²) in continuous mode (p=0.01 compared to control, Mann-Whitney U-test; ***Fig. 6B***).

Effects of combined exposure to chlorin E6 and laser irradiation in different modes on U251 human GB cell cultures and HEK293 cell lines. In U251 cell cultures, after 24-h incubation with chlorin E6 (1 μg/mL) followed by LI (0.4 W, 10 J/cm², continuous and pulse mode), retraction of the growth zone and a significant decrease in cell monolayer density occurred ***(Fig. 7A, 7B)***. The cells in the growth zone were characterized by high permeability to the vital dye (trypan blue), even at the nucleus, indicating membrane integrity damage. Under the same conditions, the density of the cell monolayer in HEK293 cell cultures also decreased significantly, with some cells losing contact with each other and the surface, becoming rounded **(Fig. 7C, 7D)**. However, only some HEK293 cells (mainly rounded, necrotized, floating ones) stained with trypan blue. In the cells of the HEK293 line, the accumulation of lipid droplets in the cytoplasm was observed, which caused cellular cytotoxicity.

Similar changes described in cells of both cell lines were observed after 24-h incubation with chlorin E6 (1 μg/mL) followed by LI (0.4 W, 25 J/cm², continuous and pulse mode) ***(Fig. 7)***.

When exposed to LI of higher power (0.6 W, 10 J/cm², continuous mode), cultures of U251 cell line showed a marked depletion of the growth zone, with cells degenerating, rounding, and losing processes ***(Fig. 7A)***. Small complexes of spread cells with processes that lost their characteristic shapes remained in the field of view, among them were bi- and tri-nucleated cells. In the growth zone of HEK293 cells under the same conditions, areas of depletion were observed, with cells losing contact with each other and the surface, leading to desquamation. A large number of rounded cells at various stages of degeneration were observed in the field of view ***(Fig. 7C)***.

When exposed to LI (0.6 W, 10 J/cm², pulse mode), U251 cells underwent degenerative changes: loss of processes, decreased adhesion, loss of characteristic cell shapes, and lipid accumulation in the cytoplasm. The growth zone was depleted, leaving clusters of cells with multiple nuclei and reduced processes ***(Fig. 7B)***. Mitotic activity decreased ($p=1\cdot10^{-6}$ compared to control, p=0.59 compared to the index under continuous LI mode, Mann-Whitney U-test).

Under the same conditions, the cell density in the HEK293 growth zone remained higher, although they underwent degenerative changes: lipid accumulation, cytoplasmic vacuolization, loss of characteristic morphological features, rounding, and the presence of multiple nuclei ***(Fig. 7D)***. Similar changes occurred in the growth zone of HEK293 cell cultures with increasing laser dose irradiation to 25 J/cm² ***(Fig. 7C, 7D)***. In pulse mode, LI led to greater depletion of the growth zone and an increase in the number of degeneratively altered cells compared to continuous mode. Mitotic activity remained at a low level (p=0.003 compared to control, for both LI modes, Mann-Whitney U-test).

The use of chlorin E6 at a concentration of 2 μg/mL followed by LI with gradual increases in power and dose resulted in even more destructive changes in the cell monolayer. In U251 cell cultures, after 24-h incubation with chlorin E6 (2 μg/mL) and subsequent LI (0.6 W, 10 J/cm², continuous mode), depletion of the growth zone was observed with residual clusters of degeneratively altered cells ($p=1 \cdot 10^{-6}$ compared to control, Mann-Whitney U-test; ***Fig. 8A***). Similar consequences under these conditions were also found in HEK293 cell cultures ***(Fig. 8C)***. Pulse mode LI was associated with a tendency to intensify the identified changes (p=0.08 compared to the index for continuous LI mode, Mann-Whitney U-test).

When the irradiation dose was increased to 25 J/ cm² in both continuous and pulse modes, destruction of the growth zone with cell remnants at various stages of degeneration was observed in cultures of both studied cell lines, but with significantly lower intensity in HEK293 cell cultures ***(Fig. 8)***. Under these conditions, mitotic

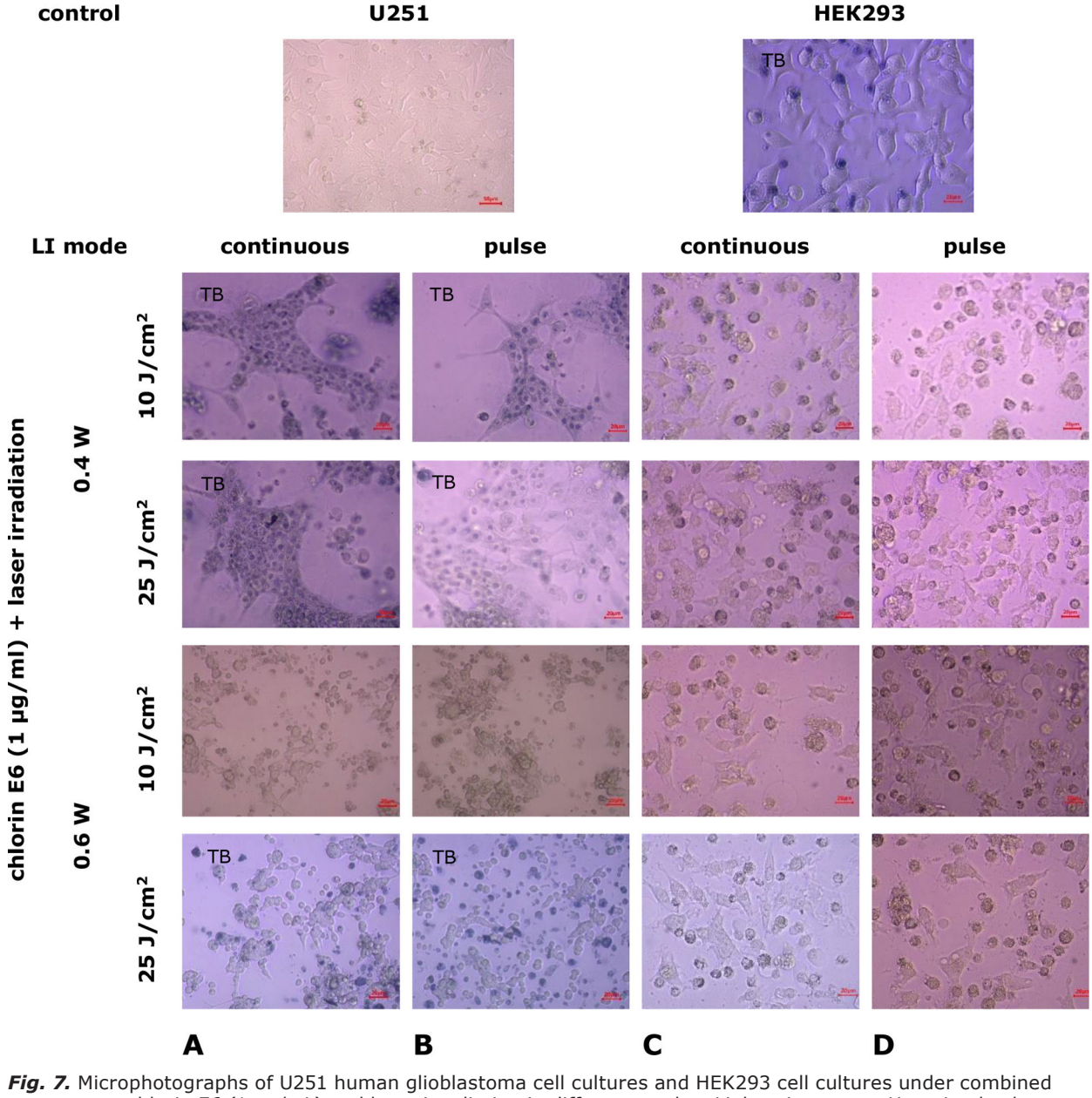

Fig. 7. Microphotographs of U251 human glioblastoma cell cultures and HEK293 cell cultures under combined exposure to chlorin E6 (1 μg/mL) and laser irradiation in different modes. Light microscopy. Unstained cultures and staining with trypan blue vital dye (TB)

activity was preserved in individual cells, especially in HEK293 lines (p=0.04 compared to control, p=0.09 compared to the index in continuous LI mode, Mann-Whitney U-test; ***Fig. 9A, 9B***).

Increasing the LI dose to 50 and 75 J/cm², in both continuous and pulse modes, slightly increased the degree of growth zone destruction in U251 cell lines. In addition to the completely destroyed areas of the growth zone, complexes and layers of adhered cells, particularly with processes, were found. However, most of these cells exhibited degenerative changes, such as loss of processes, characteristic morphological forms, cytoplasmic vacuolization, accumulation of lipid granules, and membrane integrity disruption ***(Fig. 8A, 8B)***. Similar changes in the growth zone under the same experimental conditions occurred in HEK293 cell cultures ***(Fig. 8C, 8D)***.

Mitotic activity of cells in cell cultures of U251 cell line was practically undetectable, starting from 25 J/cm² LI (0.6 W, pulse mode) ($p=3\cdot10^{-6}$ compared to control, p=0.17 compared to continuous LI mode, Mann-Whitney U-test) ***(Fig. 9A)***, whereas, in HEK293 cell cultures, mitotic activity was not recorded starting from 50 J/cm² LI (0.6 W, pulse mode) (p=0.04 compared to control, p=0.29 compared to continuous LI mode, Mann-Whitney U-test ***Fig. 9B***).

Consequently, studies on the combined effects of chlorin E6 and LI on U251 human glioblastoma cell cultures indicate a cumulative dose-dependent cytotoxic effect. Increasing the concentration of chlorin E6 from 1 to 2 μg/mL and increasing the LI power from 0.4 to 0.6 W and dose from 10 to 75 J/cm² in continuous mode consistently lead to destructive changes in the architectonics of the growth zone (these changes range from the retraction of the growth zone with the formation of lacunae of varying sizes at the lowest LI levels to gross destruction of the architectonics and significant

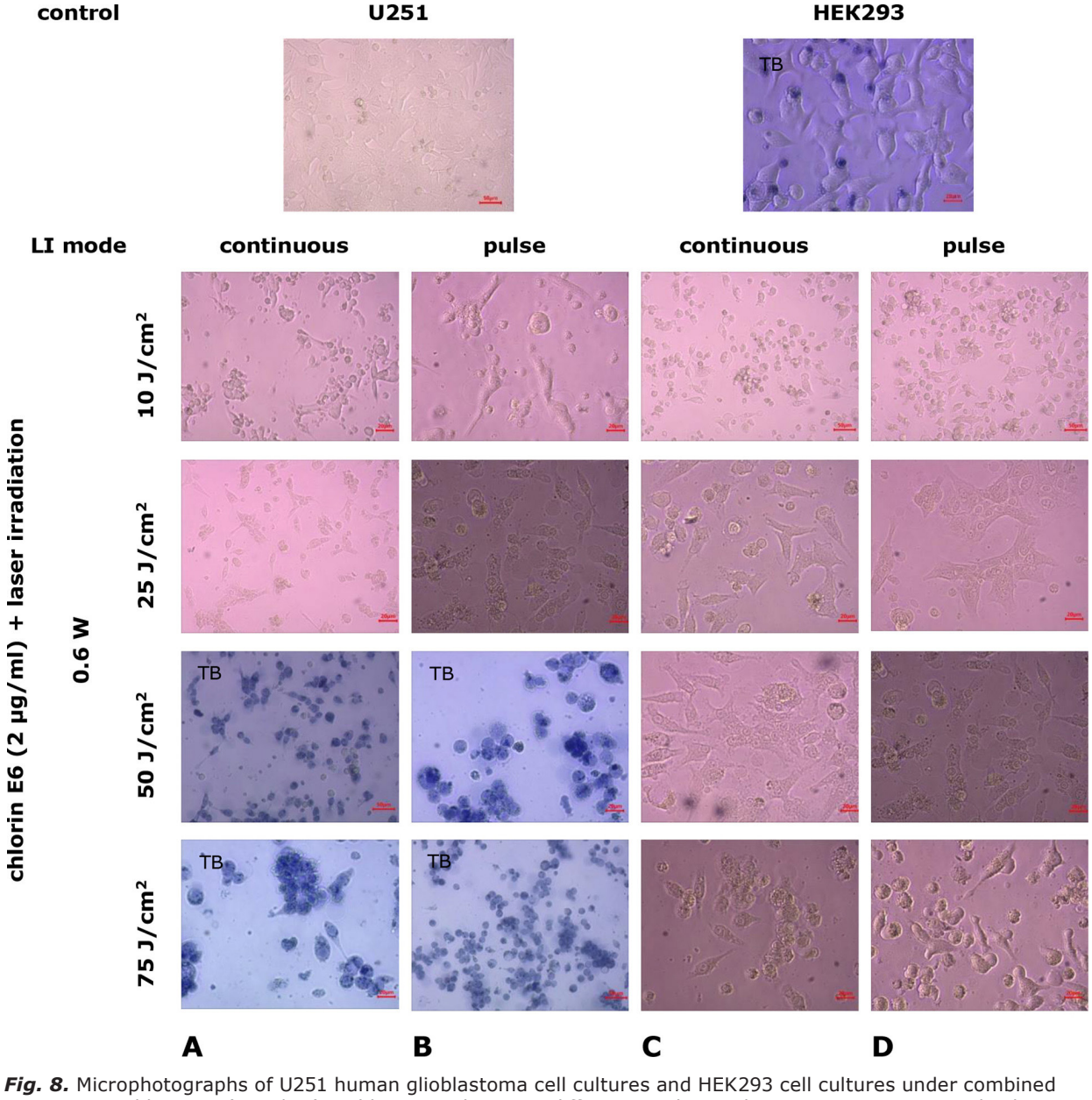

Fig. 8. Microphotographs of U251 human glioblastoma cell cultures and HEK293 cell cultures under combined exposure to chlorin E6 (2 μg/mL) and laser irradiation in different modes. Light Microscopy. Unstained cultures and staining with trypan blue vital dye (TB)

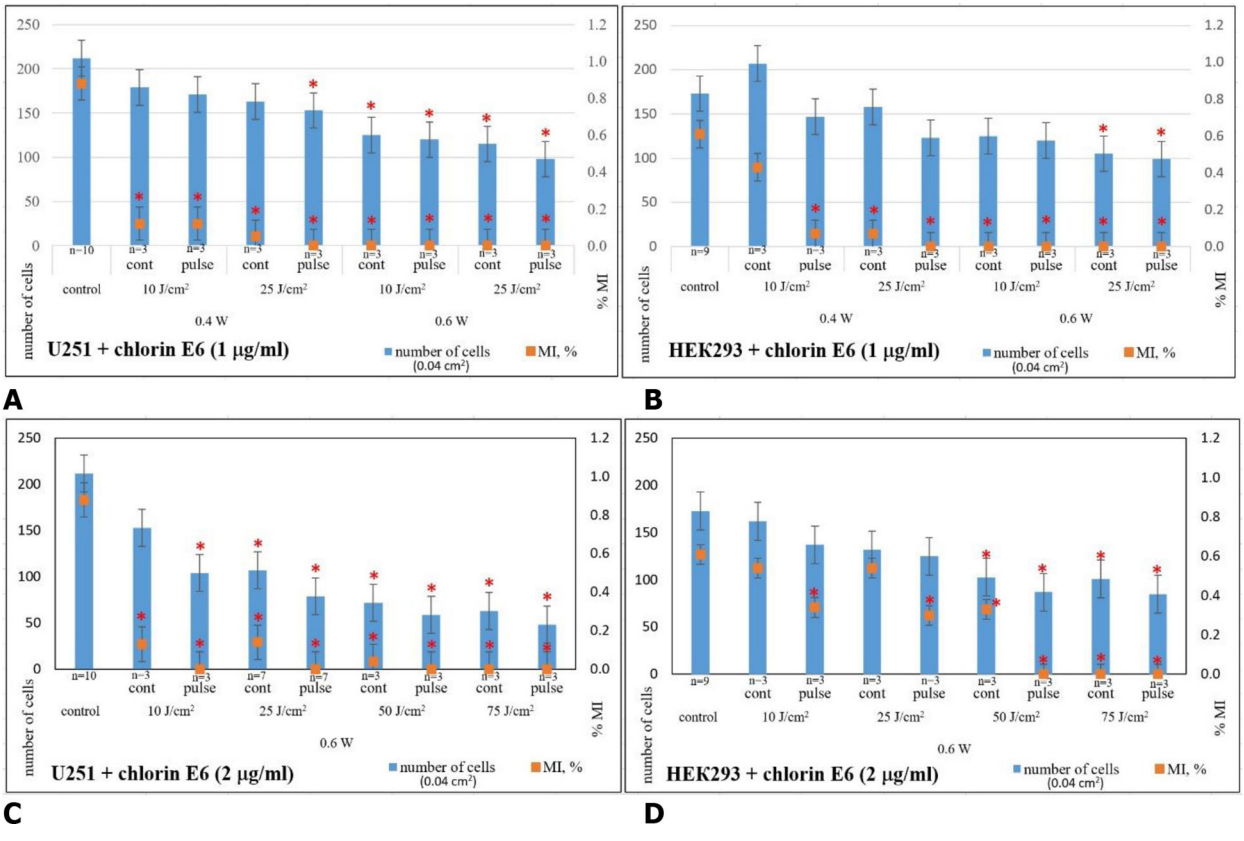

Fig. 9. Average cell count and mitotic index (MI, %) in cell cultures of U251 human GB cell line (A,C) and HEK293 cell line (B,D) 24 h after combined exposure to chlorin E6 (1 μg/mL, 2 μg/mL, 4-h pre-incubation) and various laser irradiation modes: * – $p<0.05$ compared to control; Mann-Whitney U-test

depletion of cell masses at the highest levels, as well as a dynamic reduction in the mitotic activity of tumor cells ($p=(1–3)\cdot10^{-6}$ compared to control), accumulation of necrobiotic changes, irreversible degeneration, and desquamation of dead cells. This effect tends to intensify with the use of LI in pulse mode ($p=0.37$, $p=0.17$, $p=0.45$, $p=0.50$, respectively, for LI doses of 10, 25, 50, and 75 J/ cm² compared to quantitative indicators of cultures under the combined influence of chlorin E6 and continuous LI mode, Mann-Whitney U-test). It is precisely with the combined effect of chlorin E6 (2 μg/ mL) and LI that the quantitative indicators of reduced mitotic activity in U251 human GB cell cultures become statistically significant compared to the corresponding indicators with direct LI exposure, starting at a dose of 25 J/cm² ($p=0.05$, $p=0.047$, $p=0.013$, respectively, for LI doses of 25, 50, and 75 J/cm², Mann-Whitney U-test).

The nature of the changes in HEK293 cell cultures under the combined influence of chlorin E6 and LI in the same modes is similar to that of U251 cells, but unlike tumor cells, the dynamics of the changes were not as pronounced, and their level was significantly lower. Significant pathological changes in HEK293 cells, their monolayer density, and mitotic activity were detected starting at LI mode of 0.6 W, dose of 25 J/cm² in pulse mode with the application of 1 μg/mL of chlorin E6 or LI mode of 0.6 W, dose of 50 J/cm² in pulse mode with the use of 2 μg/mL of chlorin E6. For U251 cell line, the threshold value was the following LI characteristics: power 0.4 W, dose 25 J/cm², pulse mode with the application of 1 μg/mL of chlorin E6 or power 0.6 W, dose 10 J/cm², pulse mode using 2 μg/mL of chlorin E6 ***(Fig. 9)***.

The results of the study on the combined effects of chlorin E6 (1 and 2 μg/mL, 4-h pre-incubation) and LI in various modes (λ=660 nm, power 0.4–0.6 W, dose 10–75 J/cm², continuous or pulsed mode) provide a basis for concluding the efficiency of the cytodestructive and antimitotic effects in U251 human GB cell cultures. Specifically, the application of an irradiation dose of 25 J/cm² at 0.6 W in pulse mode with chlorin E6 at a concentration of 2 μg/mL (after 4-h pre-incubation of the cell culture) is effective. The use of combined effect of PS and LI with the indicated characteristics in the culture of cells of the HEK293 cell line, which has a similar neuronal phenotype, did not entail such significant cytodestructive effects as in the culture of tumour cells of the U251 cell line, i.e. human GB cells of the line U251 are more sensitive to the photodynamic effect of chlorin E6 and LI compared to cells of the HEK293 line. One explanation for this may be the higher metabolism level of MG tumor cells compared to non-transformed cells [31, 32], as well as their faster accumulation of the photosensitizer compared to neuro cells. The selective accumulation of the PS in tumor cells is associated with low pH levels due to excess lactic acid production during active glycolysis compared to normal cells. Photosensitizers dissolve better in acidic environments and consequently accumulate more effectively in tumor cells [33].

The antimitotic effect of the applied photodynamic exposure modes using chlorin E6 in U251 human GB cell cultures is consistent with data showing reduced proliferation and clonogenic capacity in glioblastoma cell lines (T98G, MO59, LN229, U87-MG) after photodynamic exposure with the use of phthalocyanines ZnPc and TAZnPc [29].

Thus, according to the results of morphological and morphometric study, it was found that PS chlorin E6 is incorporated into the cytoplasm of human GB cell lines U251 and cells of HEK293 line, and the fluorescence intensity is comparable. The direct exposure of chlorin E6 (1.0 and 2.0 μg/ml) for 24 h dose-dependently enhanced cytodestructive and antimitotic effects in human GB culture of U251 line. In contrast to cell line U251, the cytodestructive effect of chlorin E6 on cultures of cell line HEK293 is less pronounced, but the antimitotic effect is relatively comparable in both types of cell cultures. When exposed to LI (λ=660 nm, power 0.4-0.6 W, dose 10-75 J/cm², continuous or pulse mode), cytodestructive and antimitotic effects in human GB cell culture line U251 are increased in a dose-dependent manner. The level of cytodestructive and antimitotic effects is significantly lower in cultures of the non-tumour cell line HEK293. The most significant reduction of mitotic activity of human GB cells of U251 line (~100%) was recorded at the lowest dose of LI 25 J/cm², power 0.6 W, in pulse mode, whereas for HEK293 line cells (~80%) - at LI power 0.6 W, dose 75 J/cm², in continuous mode. The combination of exposure to chlorin E6 and LI as the dose increases leads to complete destruction of tumour cells in human GB cell culture cell line U251. Total cytodestructive and antimitotic effect in the culture of human GB cell line U251 is achieved at the combination of the lowest irradiation dose 25 J/cm², power 0.6 W, in pulse mode and chlorin E6 in concentration of 2 μg/ml. In contrast to human GB cells of U251 line, the specified mode of photodynamic exposure is not irreversibly destructive for cultures of HEK293 line cells: against the background of a 1.3-fold decrease in the total number of cells, reference cells retain mitotic activity (MI~0.3%).

Consequently, human GB cells of the U251 line are more sensitive to the cumulative effect of photodynamic exposure to chlorin E6 and LI compared to HEK293 cells. An effective mode of photodynamic exposure to achieve sufficient cytodestructive and antimitotic effect in human GB cell culture of the U251 line is the combined application of irradiation with a dose of 25 J/cm², power 0.6 W, in pulse mode with pre-incubation of cell culture with chlorin E6 at a concentration of 2 μg/ml for 4 h. This mode is much less destructive, and therefore, relatively safe for cultures of HEK293 line.

Conclusions

As a result of the morphological and morphometric study, an effective photodynamic exposure has been established for achieving cytodestructive and antimitotic effects in human GB cell culture of the U251 line. The mode is relatively safe for non-malignant cells: involving the combined application of a laser irradiation dose of 25 J/cm² at 0.6 W in pulse mode, in pre-incubation of the cell culture with chlorin E6 at a concentration of 2 μg/ml for 4 h.

Acknowledgments

The authors express their sincere gratitude to Oleksandra Lykhova, Ph.D., Senior Research Fellow of the Department of Tumor Process Monitoring and Therapy Design, R.E. Kavetsky Institute of Experimental Pathology, Oncology and Radiobiology of the NAS of Ukraine, for kindly providing the U251 and HEK293 cell line samples for cultivation and research.

Disclosure

Conflict of Interest

The authors declare no conflicts of interest.

Funding

This research was not supported by any sponsorship.

The study is part of a research project (State Registration No. 0122U000331).

References

1. Sung H, Ferlay J, Siegel RL, Laversanne M, Soerjomataram I, Jemal A, Bray F. Global Cancer Statistics 2020: GLOBOCAN Estimates of Incidence and Mortality Worldwide for 36 Cancers in 185 Countries. CA Cancer J Clin. 2021 May;71(3):209-249. doi: 10.3322/caac.21660
2. Ostrom QT, Price M, Neff C, Cioffi G, Waite KA, Kruchko C, Barnholtz-Sloan JS. CBTRUS Statistical Report: Primary Brain and Other Central Nervous System Tumors Diagnosed in the United States in 2016-2020. Neuro Oncol. 2023 Oct 4;25(12 Suppl 2):iv1-iv99. doi: 10.1093/neuonc/noad149. PMID: 377931257
3. Louis DN, Perry A, Wesseling P, Brat DJ, Cree IA, Figarella-Branger D, Hawkins C, Ng HK, Pfister SM, Reifenberger G, Soffietti R, von Deimling A, Ellison DW. The 2021 WHO Classification of Tumors of the Central Nervous System: a summary. Neuro Oncol. 2021 Aug 2;23(8):1231-1251. doi: 10.1093/neuonc/noab106
4. Ostrom QT, Cioffi G, Waite K, Kruchko C, Barnholtz-Sloan JS. CBTRUS Statistical Report: Primary Brain and Other Central Nervous System Tumors Diagnosed in the United States in 2014-2018. Neuro Oncol. 2021 Oct 5;23(12 Suppl 2):iii1-iii105. doi: 10.1093/neuonc/noab200
5. Fedorenko Z, Goulak L, Gorokh Ye, Ryzhov A, Soumkina O. CANCER IN UKRAINE, 2021-2022: Incidence, mortality, prevalence and other relevant statistics. Bulletin of the National Cancer Registry of Ukraine. 2023;24. http://ncru.inf.ua/publications/BULL_24/PDF_E/bull_eng_24.pdf
6. van Solinge TS, Nieland L, Chiocca EA, Broekman MLD. Advances in local therapy for glioblastoma - taking the fight to the tumour. Nat Rev Neurol. 2022 Apr;18(4):221-236. doi: 10.1038/s41582-022-00621-0
7. Mahmoudi K, Garvey KL, Bouras A, Cramer G, Stepp H, Jesu Raj JG, Bozec D, Busch TM, Hadjipanayis CG. 5-aminolevulinic acid photodynamic therapy for the treatment of high-grade gliomas. J Neurooncol. 2019 Feb;141(3):595-607. doi: 10.1007/s11060-019-03103-4
8. Muller PJ, Wilson BC. Photodynamic therapy for malignant newly diagnosed supratentorial gliomas. J Clin Laser Med Surg. 1996 Oct;14(5):263-70. doi: 10.1089/clm.1996.14.263
9. Cramer SW, Chen CC. Photodynamic Therapy for the Treatment of Glioblastoma. Front Surg. 2020 Jan 21;6:81. doi: 10.3389/fsurg.2019.00081
10. Muragaki Y, Akimoto J, Maruyama T, Iseki H, Ikuta S, Nitta M, Maebayashi K, Saito T, Okada Y, Kaneko S, Matsumura A, Kuroiwa T, Karasawa K, Nakazato Y, Kayama T. Phase II clinical study on intraoperative photodynamic therapy with talaporfin sodium and semiconductor laser in patients with malignant brain tumors. J Neurosurg. 2013 Oct;119(4):845-52. doi: 10.3171/2013.7.JNS13415
11. Quirk BJ, Brandal G, Donlon S, Vera JC, Mang TS, Foy AB, Lew SM, Girotti AW, Jogal S, LaViolette PS, Connelly JM, Whelan HT. Photodynamic therapy (PDT) for malignant brain tumors--where do we stand? Photodiagnosis Photodyn Ther. 2015 Sep;12(3):530-44. doi: 10.1016/j.pdpdt.2015.04.009
12. Senders JT, Muskens IS, Schnoor R, Karhade AV, Cote DJ,

Smith TR, Broekman ML. Agents for fluorescence-guided glioma surgery: a systematic review of preclinical and clinical results. Acta Neurochir (Wien). 2017 Jan;159(1):151-167. doi: 10.1007/s00701-016-3028-5
13. Stummer W, Pichlmeier U, Meinel T, Wiestler OD, Zanella F, Reulen HJ; ALA-Glioma Study Group. Fluorescence-guided surgery with 5-aminolevulinic acid for resection of malignant glioma: a randomised controlled multicentre phase III trial. Lancet Oncol. 2006 May;7(5):392-401. doi: 10.1016/S1470-2045(06)70665-9
14. Kostron H, Obwegeser A, Jakober R. Photodynamic therapy in neurosurgery: a review. J Photochem Photobiol B. 1996 Nov;36(2):157-68. doi: 10.1016/s1011-1344(96)07364-2
15. Kaneko S, Fujimoto S, Yamaguchi H, Yamauchi T, Yoshimoto T, Tokuda K. Photodynamic Therapy of Malignant Gliomas. Prog Neurol Surg. 2018;32:1-13. doi: 10.1159/000469675
16. Schipmann S, Müther M, Stögbauer L, Zimmer S, Brokinkel B, Holling M, Grauer O, Suero Molina E, Warneke N, Stummer W. Combination of ALA-induced fluorescence-guided resection and intraoperative open photodynamic therapy for recurrent glioblastoma: case series on a promising dual strategy for local tumor control. J Neurosurg. 2020 Jan 24;134(2):426-436. doi: 10.3171/2019.11.JNS192443
17. Vermandel M, Dupont C, Lecomte F, Leroy HA, Tuleasca C, Mordon S, Hadjipanayis CG, Reyns N. Standardized intraoperative 5-ALA photodynamic therapy for newly diagnosed glioblastoma patients: a preliminary analysis of the INDYGO clinical trial. J Neurooncol. 2021 May;152(3):501-514. doi: 10.1007/s11060-021-03718-6
18. Eljamel MS, Goodman C, Moseley H. ALA and Photofrin fluorescence-guided resection and repetitive PDT in glioblastoma multiforme: a single centre Phase III randomised controlled trial. Lasers Med Sci. 2008 Oct;23(4):361-7. doi: 10.1007/s10103-007-0494-2
19. van Linde ME, Brahm CG, de Witt Hamer PC, Reijneveld JC, Bruynzeel AME, Vandertop WP, van de Ven PM, Wagemakers M, van der Weide HL, Enting RH, Walenkamp AME, Verheul HMW. Treatment outcome of patients with recurrent glioblastoma multiforme: a retrospective multicenter analysis. J Neurooncol. 2017 Oct;135(1):183-192. doi: 10.1007/s11060-017-2564-z
20. Lietke S, Schmutzer M, Schwartz C, Weller J, Siller S, Aumiller M, Heckl C, Forbrig R, Niyazi M, Egensperger R, Stepp H, Sroka R, Tonn JC, Rühm A, Thon N. Interstitial Photodynamic Therapy Using 5-ALA for Malignant Glioma Recurrences. Cancers (Basel). 2021 Apr 7;13(8):1767. doi: 10.3390/cancers13081767
21. Kobayashi T, Nitta M, Shimizu K, Saito T, Tsuzuki S, Fukui A, Koriyama S, Kuwano A, Komori T, Masui K, Maehara T, Kawamata T, Muragaki Y. Therapeutic Options for Recurrent Glioblastoma-Efficacy of Talaporfin Sodium Mediated Photodynamic Therapy. Pharmaceutics. 2022 Feb 2;14(2):353. doi: 10.3390/pharmaceutics14020353
22. Muller PJ, Wilson BC. Photodynamic therapy of brain tumors--a work in progress. Lasers Surg Med. 2006 Jun;38(5):384-9. doi: 10.1002/lsm.20338
23. Zavadskaya TS. Photodynamic therapy in the treatment of glioma. Exp Oncol. 2015 Dec;37(4):234-41.
24. Hamaliya MF, Shyshko YD, Shton' IO, Kholin VV, Shcherbakov OB, Usatenko OV. [Photodynamic activity of second-generation photosensitizer fotolon (chlorin e6) and its golden nanocomposite: experiments in vitro and in vivo]. Photobiology and Photomedicine. 2012;9(1-2):99-103. Ukrainian. https://periodicals.karazin.ua/photomedicine/article/view/13195
25. U-251 MG (formerly known as U-373 MG) (ECACC 09063001). Culture Collections. UK Health Security Agency; 2024. https://www.culturecollections.org.uk/products/celllines/generalcell/detail.jsp?refId=09063001&collection=ecacc_gc
26. HEK293 (ECACC 85120602). Culture Collections. UK Health Security Agency; 2024. https://www.culturecollections.org.uk/nop/product/293
27. Lin YC, Boone M, Meuris L, Lemmens I, Van Roy N, Soete A, Reumers J, Moisse M, Plaisance S, Drmanac R, Chen J, Speleman F, Lambrechts D, Van de Peer Y, Tavernier J, Callewaert N. Genome dynamics of the human embryonic kidney 293 lineage in response to cell biology manipulations. Nat Commun. 2014 Sep 3;5:4767. doi: 10.1038/ncomms5767
28. Stepanenko AA, Dmitrenko VV. HEK293 in cell biology and cancer research: phenotype, karyotype, tumorigenicity, and stress-induced genome-phenotype evolution. Gene. 2015 Sep 15;569(2):182-90. doi: 10.1016/j.gene.2015.05.065
29. Velazquez FN, Miretti M, Baumgartner MT, Caputto BL, Tempesti TC, Prucca CG. Effectiveness of ZnPc and of an amine derivative to inactivate Glioblastoma cells by Photodynamic Therapy: an in vitro comparative study. Sci Rep. 2019 Feb 28;9(1):3010. doi: 10.1038/s41598-019-39390-0
30. Rozumenko VD, Liubich LD, Staino L.P., Egorova D.M., Vaslovych VV, Rozumenko AV, Komarova OS, Dashchakovskyi AV, Kluchka VM, Malysheva TA. Effects of photodynamic exposure using chlorine E6 on U251 glioblastoma cell line in vitro. Ukrainian Neurosurgical Journal. 2023; 29(2): 11-21. doi: 10.25305/unj.273699
31. Márquez J, Alonso FJ, Matés JM, Segura JA, Martín-Rufián M, Campos-Sandoval JA. Glutamine Addiction In Gliomas. Neurochem Res. 2017 Jun;42(6):1735-1746. doi: 10.1007/s11064-017-2212-1
32. Rivera JF , Sridharan SV , Nolan JK , Miloro SA , Alam MA , Rickus JL , Janes DB . Real-time characterization of uptake kinetics of glioblastoma vs. astrocytes in 2D cell culture using microelectrode array. Analyst. 2018 Oct 8;143(20):4954-4966. doi: 10.1039/c8an01198b
33. Moan J, Peng Q. An outline of the history of PDT. Patrice T, editor. Photodynamic Therapy. London: The Royal Society of Chemistry; 2003. p. 1–18. doi: 10.1039/9781847551658-00001